



Mechanisms behind the metabolic flexibility of an invasive comb jelly



Starrlight Augustine^{a,b,c,*}, Cornelia Jaspers^{a,d}, Sebastiaan A.L.M. Kooijman^e, François Carlotti^{b,c}, Jean-Christophe Poggiale^{b,c}, Vânia Freitas^{f,g}, Henk van der Veer^g, Lodewijk van Walraven^g

^a Center for Ocean Life, DTU AQUA, Charlottenlund Castle, 2920 Charlottenlund, Denmark

^b Aix Marseille Université, Mediterranean Institute of Oceanography CNRS/INSU, IRD, UM 110, 13288 Marseille, France

^c Université de Toulon, Mediterranean Institute of Oceanography, CNRS/INSU, IRD, UM 110, 83957 La Garde, France

^d Helmholtz Centre for Ocean Research Kiel, Düsternbrooker Weg 20, 24105 Kiel, Germany

^e Department of Theoretical Biology, Vrije Universiteit, de Boelelaan 1087, 1081 HV Amsterdam, The Netherlands

^f CIMAR/CIIMAR – Centro Interdisciplinar de Investigação Marinha e Ambiental, Universidade do Porto, Rua dos Bragas 289, 4050-123 Porto, Portugal

^g Royal Netherlands Institute for Sea Research, P.O. Box 59, 1790 AB Den Burg Texel, The Netherlands

ARTICLE INFO

Article history:

Received 9 May 2014

Received in revised form 11 September 2014

Accepted 18 September 2014

Available online 24 October 2014

Keywords:

Dynamic Energy Budget Theory

Mnemiopsis leidyi

Growth

Reproduction

Development

Metabolic Acceleration

ABSTRACT

Mnemiopsis leidyi is an invasive comb jelly which has successfully established itself in European seas. The species is known to produce spectacular blooms yet it is holoplanktonic and not much is known about its population dynamics in between. One way to gain insight on how *M. leidyi* might survive between blooms and how it can bloom so fast is to study how the metabolism of this species actually responds to environmental changes in food and temperature over its different life-stages. To this end we combined modelling and data analysis to study the energy budget of *M. leidyi* over its full life-cycle using Dynamic Energy Budget (DEB) theory and literature data.

An analysis of data obtained at temperatures ranging from 8 to 30 °C suggests that the optimum thermal tolerance range of *M. leidyi* is higher than 12 °C. Furthermore *M. leidyi* seems to undergo a so-called metabolic acceleration after hatching. Intriguingly, the onset of the acceleration appears to be delayed and the data do not yet exist which allows determining what actually triggers it. It is hypothesised that this delay confers a lot of metabolic flexibility by controlling generation time.

We compared the DEB model parameters for this species with those of another holoplanktonic gelatinous zooplankton species (*Pelagia noctiluca*). After accounting for differences in water content, the comparison shows just how fundamentally different the two energy allocation strategies are. *P. noctiluca* has an extremely high reserve capacity, low turnover times of reserve compounds and high resistance to shrinking. *M. leidyi* adopts the opposite strategy: it has a low reserve capacity, high turnover rates of reserve compounds and fast shrinking.

© 2014 Elsevier B.V. All rights reserved.

1. Introduction

The comb jelly *Mnemiopsis leidyi* (A. Agassiz 1865) is native to the Atlantic coast of the United States of America (USA) and invasive in Europe (Costello et al., 2012). It was first accidentally introduced to the Black Sea in the 1980s from the Gulf of Mexico population. Then it was accidentally introduced to the North Sea from the north-east coast of the USA (Reusch et al., 2010).

At present, this species seems to be well established in European waters and its potential predatory effects on fish recruits and competition with zooplanktivorous fish species are of major concern. Thus there is a

continued interest to elucidate its impact on local community structure and functioning. A rather essential problem in this context is to understand and predict size and maturity structure of populations throughout the season because this relates to recruitment dynamics, timing of blooms and strategies to wait out bleak periods.

The first step is to understand individual energy budgets which can later be used for extrapolations to the population level. Reeve et al. (1989) proposed a first carbon budget for this species, but many new datasets have since been acquired. And importantly, more advanced methods exist now to perform mass and energy balancing on different types of field and laboratory data, namely the Dynamic Energy Budget (DEB) theory. In this study we combine modelling and data analysis to study in depth the energy budget of *M. leidyi* over its full life-cycle using the DEB theory and literature data.

The DEB theory is a theoretical framework which specifies metabolic organisation of all living organisms from uni-cellular bacteria to whales. The theory offers a precise formulation of which metabolic processes need to be represented in order to fully quantify the energy/mass

* Corresponding author at: Center for Ocean Life, DTU AQUA, Charlottenlund Castle, 2920 Charlottenlund, Denmark.

E-mail addresses: staug@aqu.dtu.dk (S. Augustine), coja@aqu.dtu.dk (C. Jaspers), bas.kooijman@vu.nl (S.A.L.M. Kooijman), francois.carlotti@univ-amu.fr (F. Carlotti), jean-christophe.poggiale@univ-amu.fr (J.-C. Poggiale), vania.freitas@nioz.nl (V. Freitas), henk.van.der.veer@nioz.nl (H. van der Veer), lodewijk.van.walraven@nioz.nl (L. van Walraven).

budget of an animal (Kooijman, 2001; Sousa et al., 2008). The formulation of these processes and how they interact make up the standard DEB model which applies to animals (Kooijman, 2010, 2012). Parameters for this model have been estimated for many different animal species (see e.g. Kooijman and Lika, 2014, for a recent overview). A number of those species seem to accelerate their metabolism after birth (Kooijman, 2014), i.e. they seem to increase metabolic rates in connection with their development. This metabolic, or type \mathcal{M} , acceleration is newly introduced to the eco-physiological literature but might well concern a large number of animal species which warrants us mentioning it here.

In this study we estimate a set of DEB model parameters on the basis of available literature data. The data all originate from different geographical locations (US and Europe) and years (1976–2014), were obtained at different temperatures (8–31 °C) and were measured in different ways (different types of weight or length measurements). By comparing the different data to a same reference (DEB model predictions) we provide an overview of this species' energy budget. We further obtain a set of DEB model parameter values based on a sub-set of the data. Last, the new findings are discussed relative to our current understanding of the biology and ecology of *M. leidyi* and compared with that of another gelatinous holoplanktonic species, the purple mauve stinger *Pelagia noctiluca* (Forskål, 1775).

2. Setup of the DEB model

We herein briefly outline the setup of the standard DEB model extended to deal with the type \mathcal{M} metabolic acceleration introduced in the precedent section. The way metabolism is conceptualized according

to this model is presented in Fig. 1A. Arrows represent energy fluxes expressed in J d^{-1} . The energy fluxes are functions of the DEB model parameters which are listed in Table 1. The equations are listed in Section A.1, Online Appendix. Boxes represent variables: energy in food E_X (J), energy in faeces E_P (J), energy in reserve E (J), structural volume V (cm^3), cumulated energy invested in maturation E_H (J) and in reproduction E_R (J). The state variables of the individual are E , V , E_H and E_R . The total mass of the individual is the sum of the mass of reserve and of structure respectively. We assume that energy invested into reproduction is immediately released into the environment in the form of gametes and so neglect its potential contribution to the total mass. Furthermore maturity itself has no mass or energy: the investment dissipates into the environment.

The model specifies energy allocation to all of the processes over the full life-cycle as shown in Fig. 1B where we illustrate how important metabolic events are situated along a maturity gradient (thick black line). Maturity is quantified as the cumulated amount of energy in joules invested into the process of maturation. Age zero is defined as the start of development (conception) and, by definition, $E_H = 0$ J. Energy investment into maturation encompasses any expenses linked to tissue differentiation, i.e. re-organisation of body structure from tentaculate to lobate form. This is different from growth which can be conceptualized as synthesis of more of the same.

Energy invested into growth is fixed into the biomass of the organism (with some overheads), but energy invested in maturation is oxidized as metabolic work making it more difficult to quantify in practice. Nonetheless it can be quantified and it can even represent a substantial part of the energy budget (Augustine et al., 2011; Mueller et al., 2012).

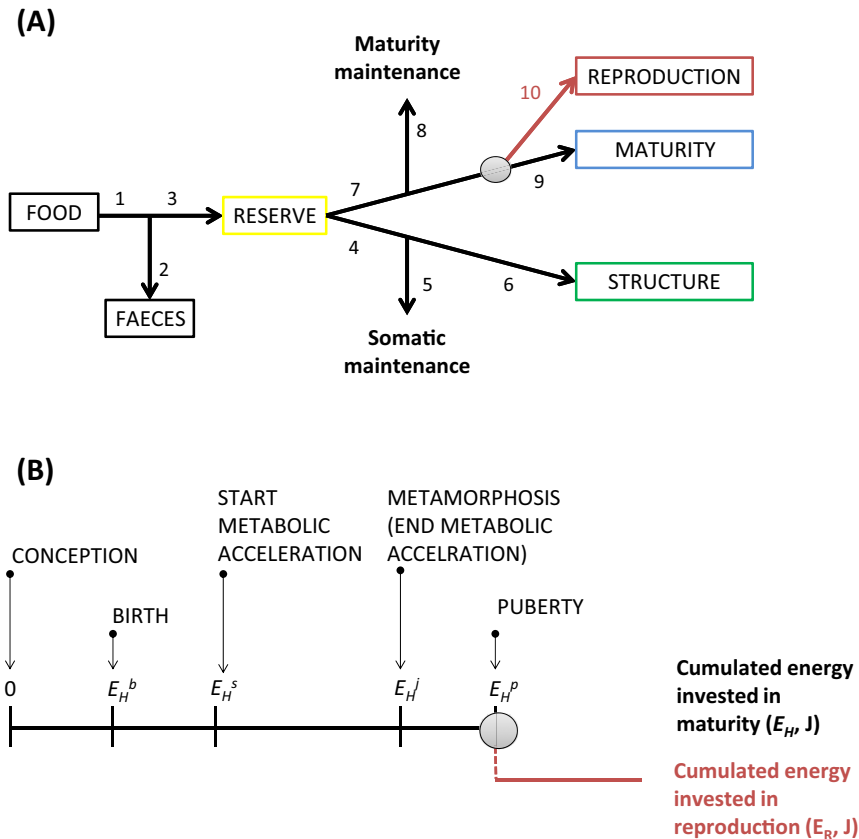


Fig. 1. Full life-cycle DEB model of the invasive comb jelly, *Mnemiopsis leidyi*. (A) DEB model scheme. Boxes: variables; arrows: energy fluxes J d^{-1} . The numbers correspond to equations given in Section A.1, Online Appendix. The state variables are food (E_X , J), faeces (E_P , J), structure (V , cm^3), reserve (E , J), maturity (quantified by the cumulated energy invested in maturation, E_H , J), and investment into reproduction (quantified as cumulated energy invested into reproduction E_R , J). Maturity and somatic maintenance costs are energy sinks. Grey circle: metabolic switch between the processes of maturation and of reproduction. (B) Definition of the different life stages in the DEB model. Between conception ($E_H = 0$) and birth ($E_H = E_H^b$) there is no external assimilation. Assimilation is switched on after birth. After birth at maturity level $E_H = E_H^b$ the organism starts metabolic acceleration which ends at metamorphosis ($E_H = E_H^j$). After puberty ($E_H = E_H^p$), i.e. the lobate adult stage, allocation towards maturation stops and allocation towards reproduction starts.

Table 1
DEB model parameters. Parameters estimated from the data (Table 2 and Fig. 2A, B) at reference temperature T_{ref} . * denotes embryo values (multiply by ca. 8.6 to obtain adult values); † denotes values which are assumed, not estimated. OA: oral–aboral, OS: oral–statocyst, total: length including lobes.

Symbol	Value	Unit	Description
$\{\dot{p}_{Am}\}$	3.0*	$\text{J d}^{-1} \text{cm}^{-2}$	Maximum surface-area specific assimilation rate
κ_X	0.8†	–	Digestion efficiency
κ_X^p	0.1†	–	Faecation efficiency
κ_R	0.95†	–	Reproduction efficiency
κ	0.7	–	Allocation fraction to soma
$[\dot{p}_M]$	5.0	$\text{J d}^{-1} \text{cm}^{-3}$	Volume linked somatic maintenance costs
$[E_G]$	78.0	J cm^{-3}	Cost of synthesis of a unit of structure
\dot{k}_J	0.002†	d^{-1}	Maturity maintenance rate coefficient
\dot{v}	0.21*	cm d^{-1}	Energy conductance
<i>Life stage parameters:</i>			
E_H^b	$1.5 \cdot 10^{-3}$	J	Cum. energy investment in maturation at birth
E_H^s	$4.4 \cdot 10^{-3}$	J	Cum. energy investment in maturation at the onset of metabolic acceleration
E_H^i	3.2	J	Cum. energy investment in maturation at metabolic metamorphosis
E_H^p	42.0	J	Cum. energy investment in maturation at puberty
<i>Temperature parameters</i>			
T_A	10,500	K	Arrhenius temperature
T_{ref}	293	K	Reference temperature
<i>Auxiliary parameters</i>			
$\delta_{\mathcal{M}}$	0.62 (OA and OS length), 0.29 (total length)	–	Shape coefficient

Birth occurs at maturity level $E_H = E_H^b$ and is defined as the moment external assimilation is initiated. This probably coincides with hatching. Puberty, is defined as the onset of adult egg production and occurs by definition at maturity level $E_H = E_H^p$. At puberty the individual stops allocating to maturation ($d E_H/dt = 0$) and starts allocating towards reproduction. This metabolic switch in energy allocation is represented by the grey circles in Fig. 1. The state variable E_R (thick red line, Fig. 1B) represents cumulated energy invested into reproduction. The model specifies energy allocation to metabolism over the full life-cycle of the organism because we include a maternal effect rule where the reserve density ($[E] = E/V$) of the neonate at birth is taken equal to that of the mother at spawning (Kooijman, 2009). Maturity levels E_H^b and E_H^p are model parameters.

As mentioned in the Introduction, a number of animal species were found to accelerate their metabolism right after birth. We include the possibility for type \mathcal{M} metabolic acceleration to occur between the maturation window $E_H^s \leq E_H \leq E_H^i$, where E_H^s and E_H^i (J) are the maturity levels where acceleration begins and ends respectively. They are also both model parameters. During metabolic acceleration both the energy conductance (\dot{v} in cm d^{-1}) and the maximum surface-area specific assimilation rate ($\{\dot{p}_{Am}\}$ in $\text{J cm}^{-2} \text{d}^{-1}$) must be multiplied by a shape correction function (Eq. A.1.1, Section A.1, Online Appendix). We refer the reader to Kooijman et al. (2011) and Kooijman (2014) for a more details concerning the shape correction function.

Maturity level E_H^i can be construed as a metabolic metamorphosis after which \dot{v} and $\{\dot{p}_{Am}\}$ take on permanent values. The ratio of pre- and post-metamorphic values is given by the acceleration factor $s_{\mathcal{M}} = L_j/L_s$ where L_s and L_j represent structural lengths at the start of the metabolic acceleration and at metamorphosis respectively.

3. Data, parameter estimation and modelling choices

We use the co-variation method of parameter estimation as defined in Lika et al. (2011) where data are divided into two categories: zero- and uni-variate. The former consist of single values which have no dependant variable (such as age at birth). The latter consist of sets of dependant and independent variables (such as length as function of time or weight as function of length).

In order to estimate parameters we collected literature data on the growth, reproduction, development, dioxygen consumption,

and ammonia and carbon dioxide excretion. All of the data which we used are collected in Section A.2, Online Appendix.

DEB theory assumes that parameters are specific to individuals although values might be similar between members of a same population or a same species. The data that exist come from a variety of different research institutions, were obtained at different years and were performed on very different populations. Thus differences between methods and ambient salinity in combination with genetic differences between populations would most likely make it impossible to fit everything with a same parameter set.

We deemed that the most rigorous first approach was to avoid making an a priori choice about which data to include or exclude from parameter estimation so at first we attempted to simultaneously fit the model to all of the different datasets that we compiled (ca. 64 datasets, see Online Appendix A.2). Our objective was to obtain DEB model parameters by fitting the DEB model to the maximum number of different types of datasets with the minimum number of parameters (Occam's razor) in order to calculate the dynamic energy budget of *M. leidyi* over its whole life-cycle in as parameter sparse and general way as possible.

Since we aimed for generality, certain species-specific characteristics were not included into the model such as the fact that ctenophores are simultaneous hermaphrodites (but see Harbinson and Miller, 1986, for exceptions) and sometimes start reproducing right after birth (Hirota, 1972; Jaspers et al., 2012, 2013; Martindale, 1987). We simply assumed reproduction starts at puberty and that energy invested into reproduction is converted to eggs with some overheads k_R . We further neglected any costs associated with the male function, but this will be addressed in more depth in the discussion.

All of the important modelling assumptions which were made when fitting the model to the data are listed in the following subsections. The consequences of these choices with respect to our results are discussed in the next section Results and discussion.

3.1. Feeding and condition

The scaled functional response f is used as a quantifier for food level. It takes value 0 for no assimilation to 1 for maximum assimilation for a given size. Some of the data were obtained from individuals sampled in the field. In that case individuals probably experienced a variety of food levels. Other data were obtained under laboratory conditions and then the authors usually aimed for ad libitum feeding conditions.

To avoid increasing the number of parameters which need to be estimated, and because we did not have more detailed information on the nutritional status of the individuals, we assumed that $f = 1$ for all of the datasets. We further assumed that the organisms were always in equilibrium with their environment meaning that the reserve density is constant: $d[E]/dt = 0$.

The scaled reserve density $e = [E]/[E_m]$ is a proxy for the individual's nutritional status (or condition). $[E_m] = \{\dot{p}_{Am}\} / \dot{v}$ is the maximum reserve density. At equilibrium $e = f$ which simplifies the equations substantially. Some of the studies also report clearance and ingestion rates. These types of measurements depend a lot on the type of food, the life stage and the experimental set-up and were not included in the current analysis. Nonetheless we still needed to specify some general digestion efficiency (κ_X) and faecation efficiency (κ_X^p) in order to compute contributions of assimilation overheads to total respiration and ammonium excretion rates in juveniles and adults. κ_X and κ_X^p are model parameters and were taken equal to 0.8 and 0.1 respectively after Lika et al. (2011).

3.2. The link between life-history and maturity levels

The reader is referred to Rapoza et al. (2005, Fig. 1) for an overview of the different life-stages: cydippid, transitional and lobate. Briefly *M. leidyi* hatches as a cydippid larvae with tentacles. During the transitional stage the tentacles regress and lobes begin to form. At the end of the transitional stage there are no more tentacles and the individual has fully formed lobes.

We need to link maturity levels to actual morphological developmental milestones if we want estimates for size and age at each milestone according to dynamic food and temperature (Augustine et al., 2011). We took the maximum size at puberty reported in the literature: 30 mm total length from Reeve et al. (1989). However it is more complex to know at which developmental milestone metabolic metamorphosis occurs. The observed range of oral-aboral (OA) lengths at the end of the cydippid larval stage (transitional stage), is 2 mm (Jaspers et al., 2013) to 5 mm (Martindale, 1987). The age and OA length at end of the transitional stage (so when lobes are fully formed) is also food and temperature dependant: published values range from 6 mm (Sullivan and Gifford, 2004) to 10 mm (Rapoza et al., 2005). During parameter estimation we tried to link metamorphosis either to the end of the cydippid larval stage or to the end of the transitional stage.

3.3. Lengths

Physical lengths, L_w (cm) are taken proportional to structural lengths L (cm), $L = V^{1/3}$: $L_w = L/\delta_M$ where δ_M is the shape coefficient which relates each type of length to the structural length. We included corrections for the different types of measurements. Three types of length measurements were reported in the data we analysed: OA, oral–stato-cyst (OS) and total lengths. Here, we do not distinguish between OA and OS. In reality, *M. leidyi* changes in shape during ontogeny in addition to increasing its water content (Anninsky et al., 2007; Rapoza et al., 2005; Reeve et al., 1989). One way to take changes in shape into account would have been to make δ_M a function of maturity level (or structural length) such that it decreases or increases as the organism goes from

one morphology to another. For simplicity we assume that δ_M is constant for each dataset.

3.4. Hydration and weights

There are 8 ways which weight is quantified in the literature: (1) carbon mass, (2) nitrogen mass, (3) ash-free dry mass (AFDM), (4) organic matter content, (5) salt-free dry fraction, (6) dry mass (DM), (7) wet mass (WM) and (8) displacement volume. According to DEB theory, reserve and structure respect strong homeostasis (in terms of elemental frequencies and chemical potential) even though both types of material comprise rich mixtures of monomers and polymers such water, ions, lipids, sugars and proteins (Kooijman, 2010). We modelled the water-free fraction of organic compartments and assumed that this corresponded to measurements (3–5). We took the water-free C:H:O:N in both reserve and structure (as well as food and faeces) equal to 1:1.8:0.5:0.1 after Lika et al. (2011), Table 2. This gives molecular weights of water-free reserve and structure (w_E and w_V) equal to 23.2 g mol⁻¹. Chemical potentials allow converting energies to C-mol and we took $\mu_E = \mu_V = 560$ kJ mol⁻¹ for reserve and structure respectively. We need to specify the chemical potential of food and faeces and took $\mu_X = 525$ kJ mol⁻¹ and $\mu_P = 480$ kJ mol⁻¹, also after Lika et al. (2011).

Next we assume that the specific densities of hydrated reserve and structure are equal $d_E^w = d_V^w = 1$ g cm⁻³ and that both reserve and structure have the same level of hydration. Under the assumption that $w_E = w_V$ and that both reserve and structure have the same amount of water, we can derive the specific density of the water free fraction of both compartments as $d_E = d_V = \delta_W d_V^w$ g cm⁻³ where δ_W is the observed AFDM/WM ratio. The literature reports different values for δ_W and in fact the level of hydration even changes during ontogeny. We assume that $\delta_W = 0.003$ g g⁻¹ and convert dry weights to ash-free dry weights assuming that salt represents 91% of the total dry mass after McNamara et al. (2013).

Last, we work with the very simple premise that δ_W is constant over ontogeny. This assumption can be relaxed by assuming that $d_E \neq d_V$ and/or $w_E \neq w_V$. Some of the DEB model parameters (found in Table 1) are sensitive to the hydration level. For instance, the parameter $[E_C]$ in J cm⁻³ quantifies the structure specific costs for growth and it is directly proportional to d_V . In addition, it was recently shown that $\{\dot{p}_{Am}\}$, $[\dot{p}_M]$ (volume linked somatic maintenance in J d⁻¹ cm⁻³) as well as the maturity levels also seem to change by the same factor as d_V (Lika et al., 2014a). But this coupling requires further study.

3.5. Dioxigen consumption and ammonia and carbon dioxide excretion

Dioxigen consumption as well as ammonia and carbon dioxide excretion follow from the mass balancing equations of the DEB model. Briefly, the predictions are weighted sums of assimilation, dissipation and growth. The equations can be found in the appendixes of both Mueller et al. (2012) and Augustine et al. (2014). We assumed that the contribution from assimilation was zero in all studies where organisms fasted before the measurements. The predictions assume that for each size class $f = 1$ so that mobilisation is not yet affected by the absence of food.

Table 2

Observed and predicted values for zero-variate data used in the parameter estimation routine.

Datasets (units)	Observed	Predicted	T °C	Source
Age at birth (d)	1	1	18	Jaspers (2012)
Age at puberty (d)	13	14	26	Baker and Reeve (1974)
Oral–aboral length at birth (mm)	0.4	0.6		Jaspers et al. (2013)
Oral–aboral length at metabolic metamorphosis (mm)	6–10	7		Rapoza et al. (2005), Sullivan and Gifford (2004)
Total length at puberty (mm)	30	34		Reeve et al. (1989)
Organic matter content of an egg (µg)	0.25	0.24		Anninsky et al. (2007)
Ultimate wet mass (ml)	51	54		Raw data from Jaspers (2012)

3.6. Reproduction rates

We assumed that low reproduction rates correspond to individuals of lesser condition after [Kremer \(1976a\)](#). In practice this meant fitting the model to the highest values of reproduction rates observed for each size on the assumption that food-deprived individuals of a given size will decrease (and perhaps cease) reproduction quite fast. The ambient salinity level was shown to impact reproduction rates ([Jaspers et al., 2011](#)) and so we focus on the higher salinity ranges.

3.7. Temperature

We assume that all metabolic rates in a single individual are affected by temperature in the same way, so that a change in temperature amounts to a transformation of rates using the simple Arrhenius relationship ([Kooijman, 2010](#)): $\dot{k}(T) = \dot{k}(T_{\text{ref}}) \exp\left(\frac{T_A - T}{T_A}\right)$ where \dot{k} is a rate and T , T_{ref} and T_A are the experimental, reference and Arrhenius temperatures (in Kelvin) respectively. The DEB model parameters with time in their dimension are standardized to $T_{\text{ref}} = 293 \text{ K}$ (20°C).

The Arrhenius relationship was used to correct all model predictions for rates and ages from T_{ref} to the experimental temperature. We assumed that $T = 26^\circ \text{C}$ for data by [Baker and Reeve \(1974\)](#) based on the geographical location. However this was unfortunately not explicitly specified in the original manuscript.

4. Results and discussion

We found that differences in measurements between studies and populations were too great and it was not possible to fit all of the data listed in Online [Appendix A](#), Section A.2 using a set of DEB models parameters in combination with the simplifying assumptions found in [Sections 3.2–3.7](#).

We were able to obtain a satisfactory fit to a coherent subset of all of those data: namely its overall life history (see [Table 2](#)), observed weight against length relationships ([Fig. 2A–C](#)) and reproduction rates against size ([Fig. 2D–F](#)) as well as its growth ([Fig. 2G](#)). The resulting DEB model parameters can be found in [Table 1](#).

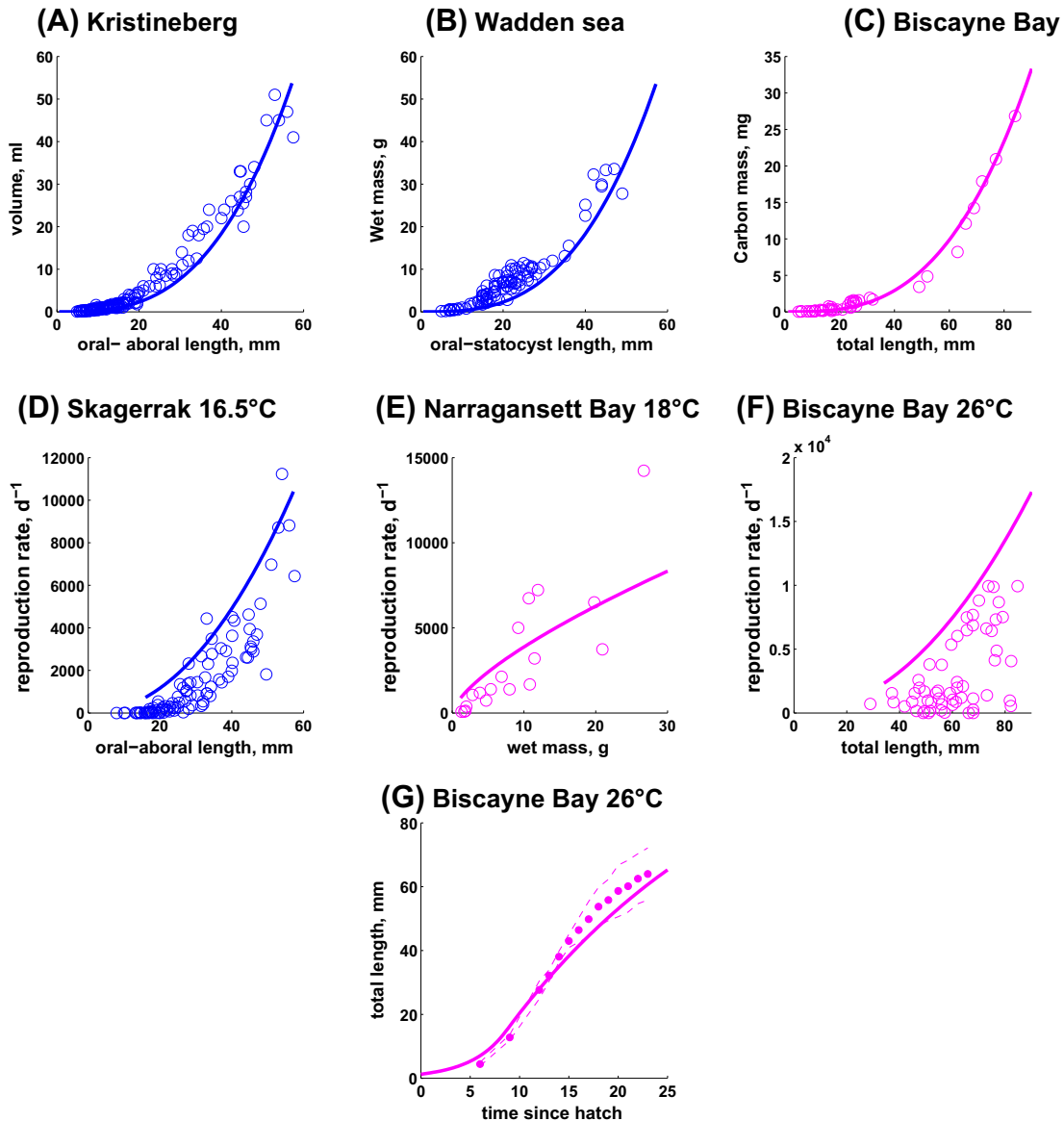


Fig. 2. Uni-variate data used to estimate DEB model parameters. Symbols: data. Solid lines: DEB model predictions assuming $f = 1$. Top row (A–C): weight length relationships from [Jaspers \(2012\)](#) (A), [van Walraven et al. \(2013\)](#) (B) and [Reeve et al. \(1989\)](#) (C). (D–F) reproduction rate length relationships from [Jaspers \(2012\)](#) (D), [Kremer \(1976a\)](#) (E) and [Baker and Reeve \(1974\)](#) (F). Finally we have the mean length against age in (G) from [Baker and Reeve \(1974\)](#), dashed lines represent the standard deviation around the mean values for the 6 individuals (circles).

In Sections 4.1–4.4 we will discuss insight gained and new questions raised through the analysis of literature data using DEB theory. The DEB model parameters in Table 1 reveal the link between energy allocation to different metabolic processes which have been computed for two relevant life-stages (Fig. 4) and key eco-physiological properties such as the organisms maximum storage capacity, the residence time of compounds in reserve and an intrinsic resistance to starvation. We will discuss this in Section 4.5 and we will further compare parameters obtained for *M. leidyi* with those of another holoplanktonic gelatinous plankton species *P. noctiluca*.

4.1. Metabolic acceleration and life history

We found that it was not possible to capture embryo development in combination with high adult reproduction rates without including metabolic acceleration. Type \mathcal{M} metabolic acceleration occurs when incubation time is longer than expected based on adult values of \dot{v} and $\{\dot{p}_{Am}\}$, length as function of age is upcurving and reserve density is not affected (Kooijman, 2014). We found that Type \mathcal{M} metabolic acceleration is needed in the first place to capture embryonic development in combination with later juvenile and adult development, growth and reproduction. Furthermore, the embryo does not show developmental arrest and cleavage is continuous (pers. obs. C. Jaspers).

We compared the DEB model predictions with several published growth curves during the cydippid and transitional stages: Anninsky et al. (2007) (28 °C), Baker and Reeve (1974) (26 °C), Reeve and Baker (1974) (21, 26 and 31 °C), Stanlaw et al. (1981) (21 °C), Sullivan and Gifford (2007) (18–21 °C) and Jaspers (2012) (19 °C). Only the DEB model prediction for length against age from Baker and Reeve (1974), used for parameter estimation, is presented graphically in Fig. 2G.

The reason that we were only able to include the growth curve from one of the studies is that larval growth presents a variety of morphologies and it is not possible to fit the model to all assuming a same scaled functional response and a same maturity level for the onset of metabolic acceleration. The growth curve from Baker and Reeve (1974) was the only one describing growth over the full life-cycle where the individuals reached their maximum size (70–80 mm total length).

Part of the explanation for why larval growth seems to be different for every study might reside in the fact that the organism changes shape as well as diet during this time (Rapoza et al., 2005; Sullivan and Gifford, 2004). However, our results also suggest that differences in timing of metabolic acceleration also contribute to these differences. This requires further research where growth is observed at different food levels and perhaps also for different feeding protocols. Overall, metabolism seems to accelerate at some point after birth and acceleration seems to stop before puberty. With the current parameter set (Table 1) the acceleration factor is about 8.6 and acceleration starts 2 days after birth at 0.7 mm OA length ($f = 1$, $T = 20$ °C).

In fact, this delay hints towards the possible metabolic flexibility for controlling generation time. Simulations show that at ad libitum food the metabolism starts to accelerate soon after birth and adult reproduction in the lobate stage can start as early as 2 weeks later at 26 °C. This allows us to hypothesise that if food levels and temperature are low (say $f = 0.3$, $T = 12$ °C) then first reproduction after metamorphosis can be delayed for up to a year (van der Molen et al., submitted for publication). However, it has been shown that several ctenophore species, both cydippid and lobate, reproduce in the cydippid larval stage (Chun, 1892; Jaspers et al., 2012; Martindale, 1987) and it has been suggested by empirical data and modelling that this is a life history trait unique to ctenophores which enables populations to maintain themselves under high predation pressure (Jaspers et al., 2012). Further studies on larval population dynamics are necessary to investigate if animals can be trapped in the larval stage as suggested by DEB model and this parameter set or not.

Resource use and its acquisition are uncoupled in the DEB model because food is first assimilated into a reserve before being mobilised

towards different metabolic processes. We compare the energy allocation of a small individual who just started accelerating against that of an individual at puberty in Fig. 4. The bar charts show what fraction of energy mobilised is allocated to each process as specified by the DEB model. From there we see that smaller individuals need to pay a factor 2 less maintenance relative to large individuals. This would be a highly ecologically relevant feature because small larvae can last a very long time at low food levels. One hypothesis is that the onset of metabolic acceleration might be triggered by an environmental factor and that delaying metabolic acceleration until food and temperature conditions are more favourable could help surviving periods without much food. A recent study on fish larvae suggests that this is the reason similar taxa of fish may or may not accelerate. The occurrence of metabolic acceleration was linked to the timing of spawning and whether or not conditions at hatch are favourable for growth (Lika et al., 2014b).

The DEB model assumes an instantaneous switch from maturing to allocating to reproduction. However, in several studies, reproductive output of ctenophores has been shown to start at low rates after puberty (Baker and Reeve, 1974; Jaspers, 2012) and is hence poorly described by the DEB model. With the current parameter set in Table 1, the model predicts that full reproduction occurs 11 days after completed metamorphosis ($f = 1$, $T = 20$ °C). However, Jaspers (2012, Chap. 6) observed that the onset of slow reproduction coincided with the completed metamorphosis of *M. leidyi* from transitional to fully lobate animals, while both Baker and Reeve (1974) and Reeve et al. (1989) reported that first reproduction occurs later than the finished metamorphosis to adult lobate stage. Thus it is still hard to ascertain how morpho-anatomical transformations relate to puberty as defined by the DEB model and perhaps this even differs between American and European populations.

The initial slow start of reproduction might also relate to investing in the male function. At puberty, investment into reproduction represents 28% of the energy mobilised from reserve while overheads linked to gamete formation comprise 2% of the total amount mobilised (Fig. 4). It is still unclear what fraction of the energy budget is invested into the male function. We interpret the above described discrepancies between model and data as evidence that it might represent more than the 5% reproduction overheads. A recent DEB modelling study on the simultaneous hermaphrodite *Limnea stagnalis* suggests that investment into the male function might represent up to 50% of the energy allocated towards reproduction (Zimmer et al., 2014). The authors also show that the investment can be modulated by environmental factors.

4.2. Reproduction rates and weight-length relationships

In Fig. 2A–C we present DEB model predictions for three weight-size relationships: volume against OA length, WM against OS length and carbon mass against total length. Overall the predictions are in the ballpark of the observed values although predictions for intermediate size classes are closer to the lower values observed.

One interpretation of the shape coefficient is that $\delta_M = L/L_w$. Thus, increasing δ_M results in increasing structural length relative to physical length; decreasing δ_M results in increasing the physical length relative to structural length. During parameter estimation we used a constant value for δ_M ; it is very likely that δ_M changes over ontogeny. Indeed, shape does change over ontogeny and a same shape coefficient might not apply for cydippid and transitional juveniles as for lobate adults. If we present cumulative number of eggs and length against time since hatch for the 6 individual ctenophores from Baker and Reeve (1974, Table 2), then the individual who reached the largest size does not have the highest cumulative egg production (not shown). This could relate to a distortion of the length measurement which might no longer be proportional to structure.

It is also likely that reserves contribute somehow to total length since lobes shrink first during starvation (pers. obs. C. Jaspers, unpublished van Walraven 2014). The predictions for carbon and nitrogen weights against OA length from Sullivan and Gifford (2004) match observed values up to 6 mm, but predictions exceed the observed values after that (not shown). However the organism changes shape around that size and we did not adjust δ_M for changes in shape within a study.

Model predictions for reproduction rate at 16.5 °C are consistent with the highest values for 30–60 mm OA length individuals (Fig. 2D). However predictions exceed the observed values for individuals less than 30 mm. The predicted reproduction rates for a given wet mass at 18 °C fall midway between the observed higher and lower boundaries (Fig. 2E). The DEB model over predicts reproduction rates against total length reported in Baker and Reeve (1974) (Fig. 2F). However the temperature in the field was not reported and we assumed that it was 26 °C. The reproduction rate against length data from Jaspers et al. (2011) taken at 12.5 °C (Kattegat, October 2009) suggest that the performance of those individuals differs notably from that of the first two datasets, but this is discussed in more detail in the following subsection.

4.3. Thermal tolerance

In order to compare the value of the Arrhenius temperature obtained in this study with Q_{10} values provided in the literature on *Mnemiopsis* we can make use of the following relationship: $Q_{10} = \exp\left(\frac{10 T_A}{T(T+10)}\right)$ (Kooijman, 2010). Thus with $T_A = 10.5$ kK, the Q_{10} is 3.5, 3.3 and 3.1 at 12, 18 and 26 °C respectively. This is within the range of values reported by Kremer (1977) and *M. leidyi* does have a very broad temperature tolerance of 2 till over 30 °C (Costello et al., 2006; Purcell et al., 2001). However what the optimal temperature range and how metabolic rates are affected by temperature outside of that range is unclear at the moment. The simple Arrhenius relationship only applies within the thermal tolerance range. Above or below the upper and lower

boundary physiological performance starts to deviate from that predicted by the relationship, the idea being that the organism is somehow stressed.

The DEB model predictions for reproduction rates against size at 16.5 and 18 °C are within the observed range (Fig. 2D–E). However the reproduction rates of individuals caught in the Kattegat at 12.5 °C (Jaspers et al., 2011) cannot be captured with this T_A (not shown). A T_A of about 25 kK as opposed to 10.5 kK reported in Table 1 would be required to capture differences between reproduction rates between studies. Such a high T_A does not fit well with a lot of the other datasets and we do not know of studies on other organisms where such a high value has been recorded.

In short, the current results suggest that 12.5 °C might already be below the optimal temperature window. This highlights the need to perform more detailed physiological experiments to assess the optimum temperature tolerance window. The current modelling framework will help in this endeavour because it will be important to take into account the combined effects of both food and temperature on physiological rates. We further detail why in the following subsection.

4.4. Respiration and excretion rates

The respiration and excretion rates were not included in the parameter estimation since values across studies showed some discrepancies as will be discussed herein. Using the parameters (Table 1) estimated simultaneously from data presented in Table 2 and Fig. 2 we computed predictions for ammonia excretion at three different temperature classes from Nemazie et al. (1993) (Fig. 3A–C) as well as dioxygen consumption at 4 temperature classes from Lilley et al. (2014) (Fig. 3D–G). In line with the original protocol we excluded contributions from assimilation from the predictions for data from Lilley et al. (2014), Kremer (1976a) and Kremer (1982). The model predictions are in line with ammonia excretion as function of dry mass from Nemazie et al. (1993). However the model overestimates the dioxygen

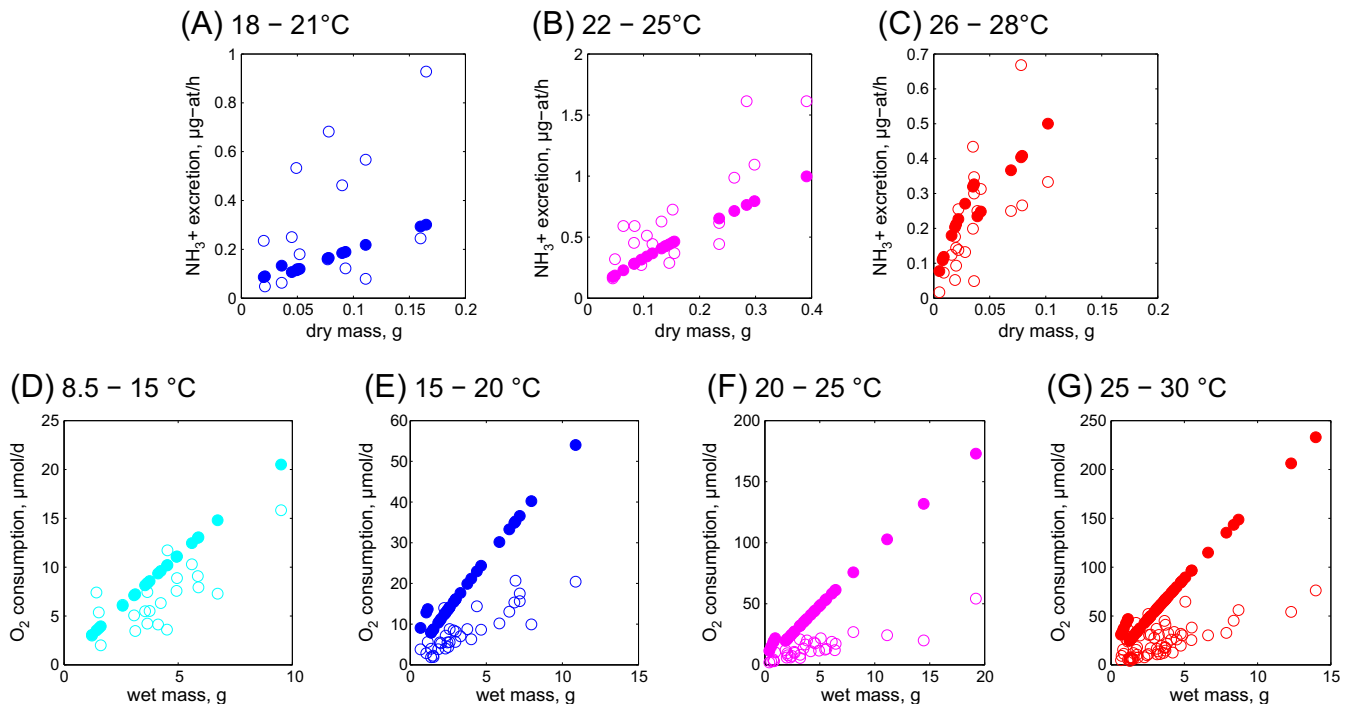


Fig. 3. Predicted ammonia excretion and dioxygen consumption as function of dry (top row) or wet (bottom row) weight. Empty symbols: data from the literature. Full symbols: DEB model predictions assuming highest possible condition factor for each size (i.e. $f = 1$). Top row (A–C): data from Nemazie et al. (1993). The DEB model predictions account for contribution from assimilation to total ammonia excretion. Bottom row (D–G): data from Lilley et al. (2014). The DEB model prediction excludes contributions from assimilation to total dioxygen consumption.

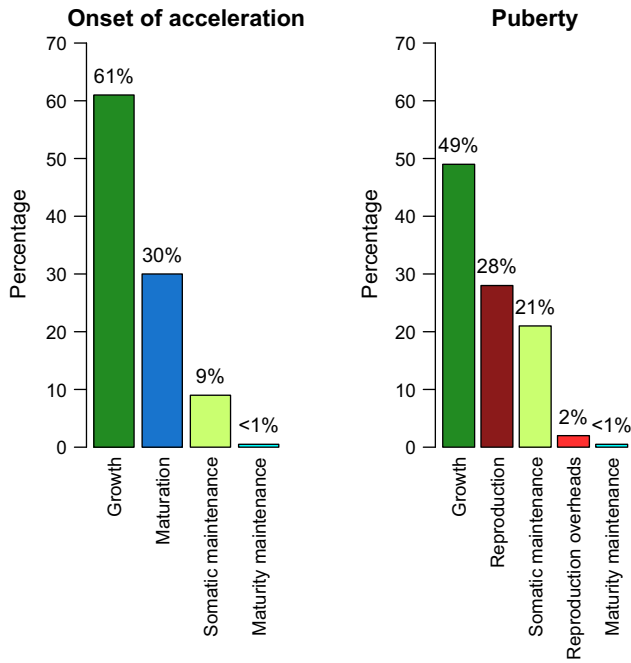


Fig. 4. Percentage of energy mobilised from reserve towards each physiological process at the onset of metabolic acceleration (left) and at puberty (right).

consumption measured in Lilley et al. (2014) for organisms above 3 g (Fig. 3D–G). Of importance to note is: the higher the temperature, the higher the discrepancy. The DEB model also over-predicts carbon dioxide, ammonia and dioxygen excretion and consumption rates reported in Kremer (1976b, Appendix) and in Kremer (1982) (not shown).

Nemazie et al. (1993) suggest that the differences between their values and that recorded in Kremer (1976a) stem from differences in contribution of organic matter to total dry mass which in turn are the result of differences in ambient salinity between studies. Nemazie et al. (1993) worked at an ambient salinity of 6–12 while Kremer and co-workers performed studies on organisms near the open ocean and Key Biscayne so the ambient salinity was probably closer to 35 (pers. comm. P. Kremer). But these difference might also stem from the fact that the metabolism of large size classes is very sensitive to short term fasting relative to that of the small size classes and that the problem is more severe the higher the temperature. The reason that larger sizes classes suffer more from food shortage is that a higher percentage (relative to a smaller individual) of energy mobilised from reserve must be allocated to cover somatic maintenance costs (see Fig. 4).

Thus at high temperatures and when measuring metabolic rates on large individuals it would probably be hard to detect the upper thermal tolerance limit without including both effects of food and temperature on physiological rates in a mechanistic way as done in this study. This might also explain why the DEB model systematically over estimates respiration and excretion rates for many of the studies while it does not for Nemazie et al. (1993) (who only worked with small size classes).

We must bear in mind that the model assumes no effect of temporary fasting on the rate of reserve mobilisation prior to the measurements (Section 3.5). There is some empirical support that short term starvation does affect the slope of dioxygen consumption over time in *Oithona davisae* where the dioxygen consumption rate is first fast then slow over the experimental period for starved nauplii (Almeda et al., 2011, Fig. 2B).

4.5. Inter-species comparison of parameter values

Of interest to note here is that the different parameters each have a specific physiological interpretation. Patterns in values for hundreds of

animal species are being studied across taxa to try and ultimately link eco-physiological properties to specific combinations of parameters values (Lika et al., 2014a). Parameters for the standard DEB model for all of these animal species can be found in the online library of DEB model parameters: the Add_my_Pet collection, http://www.bio.vu.nl/thb/deb/deblab/add_my_pet/Species.html. The model captures quite a few aspects of the individual's energy budget very realistically. The comparison between *M. leidy* and *P. noctiluca* is interesting in that both are holoplanktonic gelatinous organisms.

M. leidy has a specific density of 0.003 g cm^{-3} while that of *P. noctiluca* is around 0.01 g cm^{-3} (Augustine et al., 2014, this special issue). Thus there is a factor 3 more water in the former species relative to the latter. After accounting for differences in water content the comparison indicates a rather severe metabolic difference: *M. leidy* seems to be comprised of 80% structure while *P. noctiluca* is comprised of 98% reserve. Volume-linked somatic maintenance costs of $5 \text{ J cm}^{-3} \text{ d}^{-1}$ might seem low compared $164 \text{ J cm}^{-3} \text{ d}^{-1}$ for *P. noctiluca* or even to the proposed 'typical' $18 \text{ J cm}^{-3} \text{ d}^{-1}$ after Lika et al. (2011). But in order to compare, $[\dot{p}_M]$ should be corrected for the water content and $[\dot{p}_M]/d_v \approx 1.7 \text{ kJ g}^{-1} \text{ d}^{-1}$. *P. noctiluca* was found to invest $15 \text{ kJ g}^{-1} \text{ d}^{-1}$ (Augustine et al., 2014), and zebrafish $2.5 \text{ kJ g}^{-1} \text{ d}^{-1}$ (Augustine et al., 2011). While the 'typical' value for a generalised animal with $d_v = 0.1$ would be $0.2 \text{ kJ g}^{-1} \text{ d}^{-1}$. Thus *M. leidy* might waste assimilates to boost metabolism and shorten generation time as suggested by the 'Waste to Hurry hypothesis' (Kooijman, 2013).

The energy conductance of 0.21 cm d^{-1} before acceleration and 1.8 cm d^{-1} afterwards for *M. leidy* is very high compared to most of the values listed in the Add_my_Pet library. \dot{v} plays an important role in embryo development but also in shaping the relationship of O_2 consumption or NH_3 as function of length and weight. The physiological interpretation is that the organism has a high mobilisation rate of its reserves and so if we come back to the previous subsection it means that the time it takes for mobilisation to be affected by fasting will be short relative to species with a lower \dot{v} , all else the same. The high \dot{v} entails a low maximum reserve capacity of about 15 J cm^{-3} or 5 kJ g^{-1} . In comparison *P. noctiluca* has 14 kJ cm^{-3} or 1400 kJ g^{-1} . A rough estimate of time till starvation can be derived by $[E_m]/[\dot{p}_M] \approx 3$ whereas *P. noctiluca* has 84 days.

5. Conclusions

In this section we highlight the three most important contributions of this study to the literature on *M. leidy*'s ecophysiology. First, *M. leidy* has a large fraction of structure relative to its reserve. We estimate somatic maintenance costs to be $5 \text{ J d}^{-1} \text{ cm}^{-3}$. This is lower than many of the values found for other animal species (Lika et al., 2011). However once we account for the very high water content in this species, maintenance costs per gram of water free structure are actually higher than many of those species.

The high somatic maintenance in combination with the high energy conductance has profound consequences for the shape of e.g. respiration rate against size (length or mass) relationships. A day of starvation for a 1 g and a 10 g wet weight individual is not equivalent in terms of how it will affect metabolic rates. The low reserve capacity means that *M. leidy* shrinks, i.e. reduces its amount of structure in response to prolonged starvation.

Second, physiological rates might already start deviating from the Arrhenius relationship around $12 \text{ }^\circ\text{C}$. A constant Q_{10} should not be used for comparing rates spanning large temperature ranges. The problem of effects of temporary starvation on the large size classes is exacerbated with increasing temperatures making it hard to detect the upper temperature range at which rates start deviating from the Arrhenius relationship.

Third, it is likely that something triggers the onset of metabolic acceleration for newly hatched individuals. Until we know more about

this, experimentalists should be aware that results from experiments might differ a lot depending on whether or not the experiment starts directly after hatch or sometime after hatch when the organism is metabolically accelerating. More dedicated study on this species intrinsic phenotypic plasticity is needed in order to assess effects of genetic differences between the different populations in Europe and the USA. Our results suggest that part of the diversity in larval growth as well as size and timing of first reproduction may stem from the delay in starting metabolic acceleration in addition to the already reported insight that dietary requirements change.

A reconstruction of the dynamics of size structure over time observed in the field in combination with the knowledge herein would be very helpful to get some idea about the condition of the individuals in the different seasons. Together with new ideas presented here on the slow initial development we might get some understanding of just how long they remain small and then how in a matter of weeks they can grow to more consequent sizes (40–60 mm OA length) and sustain high reproduction rates. The observed large variation in size classes of *M. leidy* in the field (e.g. Haraldsson et al., 2013, Fig. 7) might relate to environmental factors that affect the delay in metabolic acceleration.

Acknowledgements

This study was supported by the post-doctoral research grants Jellywatch funded by the Provence Alpes Côtés d'Azur Region, the FEDER Program (Contract # 2009-21541-34380) as well as the Danish Research Council and the HCØ-scholarship. The Centre for Ocean Life is a VKR centre of excellence supported by the Villum Foundation. In addition, part of the research of SA, JCP and FC was supported by the project "MODIMIG" (EC2CO, France). "MODIMIG" funded the PNEC programme (INSU-CNRS, 2011–2013). The authors would like to thank Fabien Lombard for helpful discussions on the physiology of *M. leidy*. Finally, the authors extend thanks to all of the participants of the DEB course 2013 for stimulating DEB theory discussions as well as to 3 anonymous reviews whose comments considerably improved this manuscript.

Appendix A. Supplementary data

Supplementary data to this article can be found online at <http://dx.doi.org/10.1016/j.seares.2014.09.005>.

References

- Almeda, R., Alcazar, M., Calbet, A., Saiz, E., 2011. Metabolic rates and carbon budget of early developmental stages of the marine cyclopid copepod *Oithona davisae*. *Limnol. Oceanogr.* 56 (1), 403–414.
- Anninsky, B.E., Finenko, G.A., Almasova, G.I., Romanova, Z.A., 2007. Somatic organic content of the Ctenophores *Mnemiopsis leidy* (Ctenophora: Lobata) and *Beroe ovata* (Ctenophora: Beroidea) in early ontogenetic stages. *Russ. J. Mar. Biol.* 33 (6), 417–424.
- Augustine, S., Gagnaire, B., Adam-Guillermin, C., Kooijman, S.A.L.M., 2011. Developmental energetics of zebrafish, *Danio rerio*. *Comp. Biochem. Physiol. A Mol. Integr. Physiol.* 159, 275–283.
- Augustine, S., Rosa, S., Kooijman, S.A.L.M., Carlotti, F., Poggiale, J.-C., 2014. Modelling the eco-physiology of the purple mauve stinger, *Pelagia noctiluca* using Dynamic Energy Budget theory. *J. Sea Res.* 94, 52–64.
- Baker, L.D., Reeve, M.R., 1974. Laboratory culture of the lobate Ctenophore *Mnemiopsis mccradyi* with notes on feeding and fecundity. *Mar. Biol.* 26, 57–62.
- Chun, C., 1892. Die Disoogenie, eine Form der geschlechtlichen Zeugung. *Festschrift zum siebzigsten Geburtstag*. Engelmann, Leipzig, Germany, pp. 77–108.
- Costello, J.H., Sullivan, B.K., Gifford, D.J., Keuren, D.V., Sullivan, L.J., 2006. Seasonal refugia, shoreward thermal amplification, and metapopulation dynamics of the ctenophore *Mnemiopsis leidy* in Narragansett Bay, Rhode Island. *Limnol. Oceanogr.* 51 (4), 1819–1831.
- Costello, J., Bayha, K., Mianzan, H., Shiganova, T., Purcell, J., 2012. Transitions of *Mnemiopsis leidy* (Ctenophora: Lobata) from a native to an exotic species: a review. *Hydrobiologia* 690 (1), 21–46.
- Haraldsson, M., Jaspers, C., Tiselius, P., Aksnes, D.L., Andersen, T., Titelman, J., 2013. Environmental constraints of the invasive *Mnemiopsis leidy* in Scandinavian waters. *Limnol. Oceanogr.* 58 (1), 37–48.

- Harbinson, G.R., Miller, R.L., 1986. Not all ctenophores are hermaphrodites. Studies on the systematics, distribution, sexuality and development of two species of *Ocyropsis*. *Mar. Biol.* 90, 413–424.
- Hirota, J., 1972. Laboratory culture and metabolism of the planktonic ctenophore, *Pleurobrachia bachei* A. Agassiz. In: Takenouti, A.Y. (Ed.), *Biological Oceanography of the North Pacific Ocean*. Idemitsu Shoten, Tokyo, pp. 465–484.
- Jaspers, C., 2012. Ecology of Gelatinous Plankton with Emphasis on Feeding Interactions, Distribution Pattern and Reproduction Biology of *Mnemiopsis leidy* in the Baltic Sea (PhD thesis) National Institute of Aquatic Resources, Technical University of Denmark.
- Jaspers, C., Møller, L.F., Kiørboe, T., 2011. Salinity GRADIENT of the Baltic Sea limits the reproduction and population expansion of the newly invaded comb jelly *Mnemiopsis leidy*. *PLoS One* 6 (8), e24065.
- Jaspers, C., Haraldsson, M., Bolte, S., Reusch, T.B.H., Thygesen, U.H., Kiørboe, T., 2012. Ctenophore population recruits entirely through larval reproduction in the central Baltic Sea. *Biol. Lett.* 8, 809–812.
- Jaspers, C., Haraldsson, M., Lombard, F., Bolte, S., Kiørboe, T., 2013. Seasonal dynamics of early life stages of invasive and native ctenophores gives clues to invasion and bloom potential in the Baltic Sea. *J. Plankton Res.* 0 (0), 1–13.
- Kooijman, S.A.L.M., 2001. Quantitative aspects of metabolic organization: a discussion of concepts. *Philos. Trans. R. Soc. B* 356 (1407), 331–349.
- Kooijman, S.A.L.M., 2009. What the egg can tell us about its hen: embryonic development on the basis of dynamic energy budgets. *J. Math. Biol.* 58 (3), 377–394.
- Kooijman, S.A.L.M., 2010. *Dynamic Energy Budget Theory for Metabolic Organization*, Cambridge.
- Kooijman, S.A.L.M., 2012. Energy budgets. In: Hastings, A., Gross, L. (Eds.), *Sourcebook in Theoretical Ecology*. University of California Press, pp. 249–258.
- Kooijman, S.A.L.M., 2013. Yolk eggs prepare for metabolic acceleration. *J. Math. Biol.* 66, 795–805.
- Kooijman, S.A.L.M., 2014. Metabolic acceleration in animal ontogeny: an evolutionary perspective. *J. Sea Res.* 94, 128–137.
- Kooijman, S.A.L.M., Lika, K., 2014. Resource allocation to reproduction in animals. *Biol. Rev.* 849–859 <http://dx.doi.org/10.1111/brv.12082>.
- Kooijman, S.A.L.M., Pecquerie, L., Augustine, S., Jusup, M., 2011. Scenarios for acceleration in fish development and the role of metamorphosis. *J. Sea Res.* 66, 419–423.
- Kremer, P., 1976a. Population dynamics and ecological energetics of a pulsed zooplankton predator, the ctenophore *Mnemiopsis leidy*. In: Wiley, M. (Ed.), *Estuarine Processes Vol. 1: Uses, Stresses and Adaptation to the Estuary*. Academic Press, pp. 197–215.
- Kremer, P.M., 1976b. The Ecology of the Ctenophore *Mnemiopsis leidy* in Narragansett Bay (PhD thesis) University of Rhode Island.
- Kremer, P., 1977. Respiration and excretion by the ctenophore *Mnemiopsis leidy*. *Mar. Biol.* 44, 43–50.
- Kremer, P., 1982. Effect of food availability on the metabolism of the ctenophore *Mnemiopsis mccradyi*. *Mar. Biol.* 71, 149–156.
- Lika, K., Kearney, M.R., Freitas, V., van der Veer, H.W., van der Meer, J., Wijsman, J.W.M., Pecquerie, L., Kooijman, S.A.L.M., 2011. The "covariation method" for estimating the parameters of the standard Dynamic Energy Budget model I: philosophy and approach. *J. Sea Res.* 66, 270–277.
- Lika, K., Augustine, S., Pecquerie, L., Kooijman, S.A.L.M., 2014a. The bijection from data to parameter space with the standard deb model quantifies the supply–demand spectrum. *J. Theor. Biol.* 357, 35–47. <http://dx.doi.org/10.1016/j.jtbi.2014.03.025>.
- Lika, K., Kooijman, S.A.L.M., Papandroulakis, N., 2014b. Metabolic acceleration in Mediterranean periciformes. *J. Sea Res.* 94, 37–46.
- Lilley, M.K.S., Thibault-Botha, D., Lombard, F., 2014. Respiration demands increase significantly with both temperature and mass in the invasive ctenophore *Mnemiopsis leidy*. *J. Plankton Res.* 36 (3), 831–837.
- Martindale, M.Q., 1987. Larval reproduction in the ctenophore *Mnemiopsis mccradyi* (order Lobata). *Mar. Biol.* 94, 409–414.
- McNamara, M.E., Lonsdale, D.J., Aller, R.C., 2013. Elemental composition of *Mnemiopsis leidy* A. Agassiz 1865 and its implications for nutrient recycling in a long island estuary. *Estuar. Coasts* 36, 1253–1264. <http://dx.doi.org/10.1007/s12237-013-9636-x>.
- Mueller, C., Augustine, S., Kearney, M.R., Kooijman, S.A.L.M., Seymour, R., 2012. The trade-off between maturation and growth during accelerated development in frogs. *Comp. Biochem. Physiol. A Mol. Integr. Physiol.* 163, 95–102.
- Nemazie, D.A., Purcell, J.E., Glibert, P.M., 1993. Ammonium excretion by gelatinous zooplankton and their contribution to the ammonium requirements of microplankton in Chesapeake Bay. *Mar. Biol.* 116, 451–458.
- Purcell, J.E., Shiganova, T.A., Decker, M.B., Houde, E.D., 2001. The ctenophore *Mnemiopsis* in native and exotic habitats: U.S. estuaries versus the Black Sea basin. *Hydrobiologia* 451, 145–176.
- Rapoza, R., Novak, D., Costello, J.H., 2005. Life-stage dependent, in situ dietary patterns of the lobate ctenophore *Mnemiopsis leidy* Agassiz 1865. *J. Plankton Res.* 27 (9), 951–956.
- Reeve, M.R., Baker, L.D., 1974. Production of two planktonic carnivores (chaetognath and ctenophore) in South Florida inshore waters. *Fish. Bull.* 73 (2), 238–248.
- Reeve, M.R., Syms, M.A., Kremer, P., 1989. Growth dynamics of a ctenophore (*Mnemiopsis*) in relation to variable food supply. I. Carbon biomass, feeding, egg production, growth and assimilation efficiency. *J. Plankton Res.* 11, 535–552.
- Reusch, T.B.H., Bolte, S., Sparwel, M., Moss, A.G., Javidpour, J., 2010. Microsatellites reveal origin and genetic diversity of Eurasian invasions by one of the world's most notorious marine invader, *Mnemiopsis leidy* (Ctenophora). *Mol. Ecol.* 19, 2690–2699.
- Sousa, T., Domingos, T., Kooijman, S.A.L., 2008. From empirical patterns to theory: a formal metabolic theory of life. *Philos. Trans. R. Soc. B* 363, 2453–2464.

- Stanlaw, K.A., Reeve, M.R., Walter, M.A., 1981. Growth, food, and vulnerability to damage of the ctenophore *Mnemiopsis mccradyi* in its early life history stages. *Limnol. Oceanogr.* 26 (2), 224–234.
- Sullivan, L.J., Gifford, D.J., 2004. Diet of the larval ctenophore *Mnemiopsis leidyi* A. Agassiz (Ctenophora, Lobata). *J. Plankton Sea Res.* 26 (4), 417–431.
- Sullivan, L.J., Gifford, D.J., 2007. Growth and feeding rates of the newly hatched larval ctenophore *Mnemiopsis leidyi* A. Agassiz (Ctenophora, Lobata). *J. Plankton Sea Res.* 29 (11), 949–965.
- van der Molen, J., van Beek, J., Augustine, S., Vansteenbrugge, L., van Walraven, L., Langenberg, V., van der Veer, H., Hostens, K., Robbens, J., 2014n. Modelling Survival and Connectivity of *Mnemiopsis leidyi* in the Southern North Sea and Scheldt Estuaries, (submitted for publication).
- van Walraven, L., Langenberg, V.T., van der Veer, H.W., 2013. Seasonal occurrence of the invasive ctenophore *Mnemiopsis leidyi* in the Western Dutch Wadden sea. *J. Sea Res.* 82, 86–92.
- Zimmer, E.I., Ducrot, V., Jager, T., Koene, J., Lagadic, L., Kooijman, S.A.L.M., 2014. Metabolic acceleration in the pond snail *Lymnaea stagnalis*? *J. Sea Res.* 94, 84–91.